



Contents lists available at SciVerse ScienceDirect

Journal of Biomechanics

journal homepage: www.elsevier.com/locate/jbiomech
www.JBiomech.com

Short communication

A rolling constraint reproduces ground reaction forces and moments in dynamic simulations of walking, running, and crouch gait

Samuel R. Hamner^a, Ajay Seth^b, Katherine M. Steele^a, Scott L. Delp^{a,b,*}^a Department of Mechanical Engineering, Stanford University, USA^b Department of Bioengineering, Stanford University, USA

ARTICLE INFO

Article history:

Accepted 30 March 2013

Keywords:

Biomechanics
Musculoskeletal
Dynamic simulation
Induced acceleration analysis
Contact model
Muscle function
Foot-ground constraints

ABSTRACT

Recent advances in computational technology have dramatically increased the use of muscle-driven simulation to study accelerations produced by muscles during gait. Accelerations computed from muscle-driven simulations are sensitive to the model used to represent contact between the foot and ground. A foot-ground contact model must be able to calculate ground reaction forces and moments that are consistent with experimentally measured ground reaction forces and moments. We show here that a rolling constraint can model foot-ground contact and reproduce measured ground reaction forces and moments in an induced acceleration analysis of muscle-driven simulations of walking, running, and crouch gait. We also illustrate that a point constraint and a weld constraint used to model foot-ground contact in previous studies produce inaccurate reaction moments and lead to contradictory interpretations of muscle function. To enable others to use and test these different constraint types (i.e., rolling, point, and weld constraints) we have included them as part of an induced acceleration analysis in OpenSim, a freely-available biomechanics simulation package.

© 2013 Elsevier Ltd. All rights reserved.

1. Introduction

Muscle-driven simulations of human gait have provided insights into the actions of muscles during walking (e.g., Anderson and Pandy, 2003; Liu et al., 2008), running (e.g., Hamner et al., 2010; Sasaki and Neptune, 2006), and pathological gait (e.g., Peterson et al., 2010; Steele et al., 2010). These studies employ methods, like induced acceleration analysis, which decompose ground reaction forces and moments using foot-ground contact models to examine how muscle forces contribute to accelerations of joints and the body mass center. Results from these studies depend upon the ground contact model (Dorn et al., 2012a; Hamner et al., 2010). It is therefore essential to assess the ability of different contact models to produce accurate ground reactions. Previous studies have compared simulated reaction forces to experimentally measured ground reaction forces (Anderson and Pandy, 2001; Dorn et al., 2012b; Seth and Pandy, 2007). It is also necessary to compare simulated reaction *moments* to measured ground reaction *moments*.

The purpose of this study was to examine the accuracy with which a rolling constraint represents contact between the foot and ground during induced acceleration analyses of walking, running, and crouch gait. Induced acceleration analysis uses a model of foot-ground contact

to determine how muscles, gravity, and velocity-related forces contribute to the ground reaction force. To test the accuracy of a rolling constraint we compared ground reaction forces and moments computed in an induced acceleration analysis to experimentally measured ground reaction forces and moments. We also evaluated other constraint-based contact models in an induced acceleration analysis of running to illustrate that these different models produce inaccurate reaction moments and lead to contradictory interpretations of muscle function.

2. Methods

We used simulations of three different gait patterns: walking (Liu et al., 2008), running (Hamner et al., 2010), and crouch gait (Steele et al., 2012) (Fig. 1). Marker trajectories and ground reaction forces and moments were measured while subjects either walked over ground or ran on a treadmill instrumented with force plates. Muscle-driven simulations were generated from these experimental data using OpenSim (Delp et al., 2007). A musculoskeletal model consisting of 92 muscles of the lower extremities and torso was scaled to match each subject's anthropometry using experimentally measured markers placed on anatomical landmarks and calculated joint centers. A corresponding virtual marker set was placed on the model based on these anatomical landmarks. Joint angles were calculated using an inverse kinematics algorithm that minimized the difference between experimental and virtual markers at each time frame (Delp et al., 2007). The computed muscle control algorithm (Thelen et al., 2003) determined muscle excitation patterns required to track measured motion. Details of experimental and simulation methods are included in the primary publications (Hamner et al., 2010; Liu et al., 2008; Steele et al., 2012).

* Correspondence to: Clark Center, Room S-321, Stanford University, Mail Code 5450, 318 Campus Drive, Stanford CA 94305-5450, USA. Tel.: +1 650 723 1230; fax: +1 650 723 8544.

E-mail address: delp@stanford.edu (S.L. Delp).

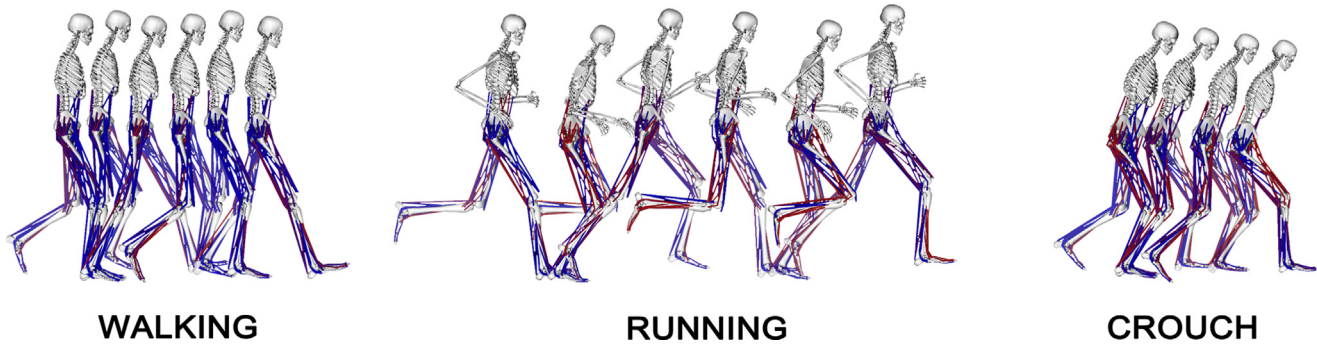


Fig. 1. Simulations of a walking gait cycle, a running gait cycle, and a crouch gait cycle. The simulations shown are of a representative subject from each study. Each set of simulations (i.e., walking, running, crouch) consisted of data from three subjects; all were analyzed using the rolling constraint to model ground contact during an induced acceleration analysis. Each simulation used a scaled musculoskeletal model with the lower extremities and torso driven by 92 musculotendon actuators.

An induced acceleration analysis was used to compute reaction forces and moments of a constraint between the foot and ground due to the forces acting on the musculoskeletal model: muscle forces, gravity, and forces due to velocity effects (i.e., Coriolis and centripetal forces). The resultant constraint reaction force and moment were calculated by summing the constraint reactions due to each force acting on the musculoskeletal model. This calculated sum was then compared to the experimentally measured ground reaction force and moment to assess accuracy.

We calculated accelerations due to forces acting on the musculoskeletal model using equations of motion for a constrained, rigid body system with muscles (Sherman et al., 2011):

$$[M]\ddot{q} + [C]^T\lambda = [R]F_m + F_g + F_v \quad (1)$$

$$[C]\dot{q} = b \quad (2)$$

where M is the mass matrix, q is a vector of generalized coordinates (e.g., joint angles), C is the constraint matrix, λ represents generalized constraint reaction forces, F_m represents muscle forces, F_g represents gravitational forces, F_v represents forces due to velocity effects, R is the matrix of muscle moment arms, and b is a vector containing position and velocity terms (i.e., q and \dot{q}) of the constraint equations (i.e., Eqs. (3)–(6)) expressed in terms of generalized accelerations, \ddot{q} . The constraint matrix C maps generalized constraint reaction forces λ to generalized accelerations \ddot{q} and generalized accelerations \ddot{q} are solved simultaneously.

To model contact between the foot and ground, we implemented a rolling constraint (Fig. 2; ROLL) that generates a fore-aft, vertical, and mediolateral reaction force and a vertical reaction moment. With a constraint-based contact model, constraint equations are included in the equations of motion and reactions are computed at each time step. Contact models utilizing spring-dampers (e.g., Anderson and Pandey, 2001; Neptune et al., 2000) require equations of motion to be integrated forward in time to calculate contact forces. Constraint-based models eliminate the computational cost of forward integrations and sensitivity of results due to differing integration time windows.

The rolling constraint combines four individual constraints: a unilateral non-penetrating constraint (Eq. (3); i.e., foot cannot penetrate ground but can be lifted) and a pure rolling constraint (Kane, 1961) (Eqs. (4)–(6)), which includes two no-slip constraints (i.e., limits fore-aft and mediolateral foot translations) and a no-twist constraint about the axis normal to ground (i.e., limits vertical rotations). Each constraint is applied at the measured center of pressure.

Constraint name	Equation	Constraint condition(s)	
Vertical, unilateral, non-penetrating	$\rho_Y(q) \geq 0$	$\hat{F}_Y > F_{threshold}$	(3)
Fore-aft no slip	$v_X(q, \dot{q}) = 0$	non-penetrating condition and $\hat{F}_Y \mu_{friction} > \sqrt{F_X^2 + F_Z^2}$	(4)
Mediolateral no slip	$v_Z(q, \dot{q}) = 0$	non-penetrating condition and $\hat{F}_Y \mu_{friction} > \sqrt{F_X^2 + F_Z^2}$	(5)
Vertical no-twist	$\omega_Y(q, \dot{q}) = 0$	no slip condition and $r_{contact} \mu_{friction} \hat{F}_Y > M_Y$	(6)

In Eqs. (3)–(6), ρ_Y is the vertical position of the foot, v_X and v_Z are the fore-aft and mediolateral foot velocities, respectively, and ω_Y is the foot's vertical angular

velocity, all with respect to ground. \hat{F}_Y is the measured vertical ground reaction force, F_X and F_Z are the simulated fore-aft and mediolateral constraint reaction forces, respectively, and M_Y is the simulated vertical constraint reaction moment. The constraint equations are differentiated to provide constraints on the system accelerations, \ddot{q} (Eq. (2)).

Specified parameters were used to determine when each constraint was active (i.e., turn on/off each constraint) based on constraint conditions in Eqs. (3)–(6). If conditions were met, each constraint was applied to the foot at the measured center of pressure, allowing direct comparison of simulated constraint reactions and measured ground reactions. In the constraint conditions, $F_{threshold}$ is a threshold (5 N) for the vertical reaction force used to determine when the non-penetrating constraint is active (Eq. (3)), $\mu_{friction}$ is a friction coefficient (0.65) used to determine when the no-slip constraints are active (Eqs. (4)–(5)), and $r_{contact}$ is a contact radius (0.01 m) representing the size of the contact area between foot and ground and is used to determine a threshold for the reaction moment (Eq. (6)). Parameter values were determined by varying each parameter within a range of physically realistic values (i.e., $0 \text{ N} < F_{threshold} < 50 \text{ N}$; $0.01 < \mu_{friction} < 1$ and $0.001 \text{ m} < r_{contact} < 0.1 \text{ m}$) and selecting values that provided appropriate timing for heel strike and toe-off. Parameters only affected when the constraints were active and varying parameters had no effect on the magnitude of reaction forces and moments calculated with the constraints. The accuracy of the rolling constraint was assessed by calculating root-mean square (RMS) difference between each component of measured ground reactions and simulated constraint reactions, averaged from the three subjects in each study.

To examine how different constraint-based contact models affect interpretation of muscle function, we conducted a case study using running simulations in which we quantified how different constraints affect muscle contributions to mass center accelerations calculated by induced acceleration analysis. We examined running as it produces larger, more rapidly changing ground reaction forces than walking. We compared the rolling constraint with two constraint-based contact models used in previous studies: a point constraint (Fig. 2; POINT) and a weld constraint (Fig. 2; WELD). The point constraint does not allow the foot to translate in any direction (i.e., fore-aft, mediolateral, or vertical), while it allows the foot to rotate about all three axes (e.g., Kepple et al., 1997). Thus, a point constraint applied at the center of pressure generates reaction force in all directions (i.e., F_X , F_Y , and F_Z), but cannot generate any reaction moment (i.e., M_X , M_Y , and M_Z). The weld constraint does not allow the foot to translate or rotate (e.g., Anderson and Pandey, 2001) and can thus generate reaction forces and moments in all directions. By comparison, the rolling constraint limits foot translation in all directions while only limiting rotation about the vertical axis, thus generating reaction forces in all directions but only a vertical reaction moment. Each constraint (ROLL, POINT, and WELD) was applied in the same induced acceleration analysis framework, allowing for direct comparison between simulated constraint reactions and measured ground reactions. The point and weld constraints were turned on when the vertical ground reaction force exceeds a specified threshold (i.e., $\hat{F}_Y > F_{threshold}$). Accuracy of each constraint type was assessed by calculating RMS difference between each component of average simulated constraint reactions and average measured ground reactions. We also calculated average contributions of soleus and vasti to fore-aft and upward mass center accelerations during stance, as these represent important muscle groups for braking and propulsion (Hamner et al., 2010; Liu et al., 2008; Neptune et al., 2008).

3. Results

The rolling constraint produced reaction forces and moments similar to ground reaction forces and moments measured about the center of pressure for walking, running and crouch gait (Fig. 3). In each case, muscles of the lower extremities and torso, gravity,

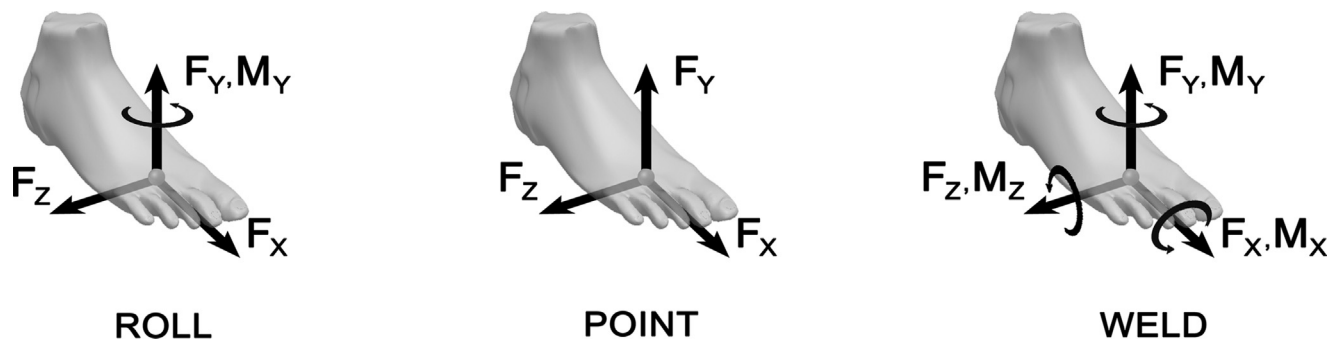


Fig. 2. The rolling constraint (ROLL) generates a fore-aft (F_x), vertical (F_y), and mediolateral (F_z) reaction force and the vertical reaction moment (M_y) about the center of pressure. The POINT constraint can only generate a fore-aft, vertical, and mediolateral reaction force. The WELD constraint can generate a fore-aft, vertical, and mediolateral reaction force and a frontal (M_x), vertical (M_y), and sagittal (M_z) reaction moment about the center of pressure.

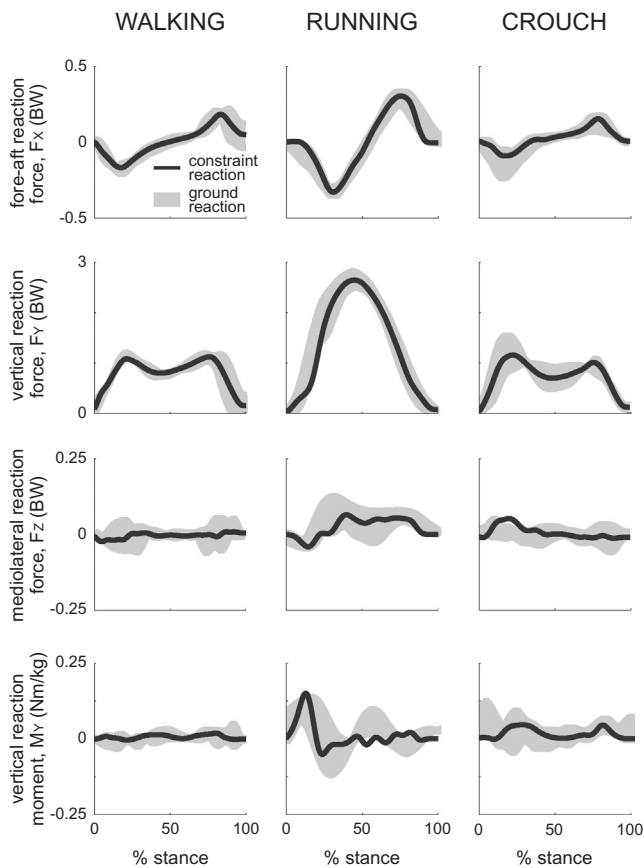


Fig. 3. Comparison of the simulated constraint reaction forces and moments (black) with the experimentally measured ground reaction forces and moments (gray) for walking, running, and crouch gait using the rolling constraint (ROLL). The shaded region represents the mean \pm one standard deviation of the measured ground reactions for three subjects included in each study.

and forces due to velocity effects accounted for more than 95% of the ground reaction force and moment. The rolling constraint, by design, only produced a vertical reaction moment when applied at the center of pressure. Analysis of running produced the largest difference between simulated constraint reactions and measured ground reactions, with a maximum RMS difference of 0.08 body weights in vertical reaction force and 0.04 Nm/kg in vertical reaction moment (Table 1).

The point constraint reproduced measured ground reaction forces with a maximum RMS difference of 0.09 body weights in vertical reaction force (Table 2), but did not generate any reaction moment because it does not constrain foot rotation (Fig. 4,

Table 1

RMS difference between each component of the simulated constraint reaction and experimentally measured ground reaction force and moment, as calculated about the center of pressure, for three different types of gait (walking, running, and crouch) using the rolling (ROLL) constraint. The ground reaction force is normalized by body weights (BW), and the ground reaction moment is normalized by body mass (Nm/kg). Note that the RMS difference of M_x and M_z for the rolling constraint during walking, running, and crouch is essentially zero ($\ll 0.01$).

Gait type	F_x (BW)	F_y (BW)	F_z (BW)	M_x (Nm/kg)	M_y (Nm/kg)	M_z (Nm/kg)
WALKING	0.01	0.03	0.01	$\ll 0.01$	0.01	$\ll 0.01$
RUNNING	0.04	0.08	0.02	$\ll 0.01$	0.04	$\ll 0.01$
CROUCH	0.03	0.03	0.02	$\ll 0.01$	0.02	$\ll 0.01$

Table 2

RMS difference between each component of the simulated constraint reaction and experimentally measured ground reaction force and moment, as calculated about the center of pressure in simulations of a single subject running over 14 consecutive gait cycles using three different constraint types (ROLL, POINT, WELD; see Fig. 2). The ground reaction force is normalized by body weights (BW) and the ground reaction moment is normalized by body mass (Nm/kg). Note that the RMS difference of M_x and M_z for the ROLL and POINT constraints is essentially zero ($\ll 0.01$).

Constraint type	F_x (BW)	F_y (BW)	F_z (BW)	M_x (Nm/kg)	M_y (Nm/kg)	M_z (Nm/kg)
ROLL	0.03	0.08	0.01	$\ll 0.01$	0.02	$\ll 0.01$
POINT	0.03	0.09	0.01	$\ll 0.01$	0.03	$\ll 0.01$
WELD	0.28	0.28	1.00	7.99	3.23	1.51

POINT). In contrast, the weld constraint generated reaction moments about all three axes because it constrains foot rotation in all directions (Fig. 4, WELD). Before toe-off, as the foot rotates, the weld constraint generated large, inaccurate forces and moments, with a maximum RMS difference of 1.0 body weight in mediolateral force and 8.0 Nm/kg in frontal reaction moment (Table 2).

Using different constraints led to different interpretations of muscle function during running. With the rolling and point constraints, vasti was the largest contributor to backward and upward mass center accelerations during early stance, while soleus was the largest contributor to forward and upward mass center acceleration during late stance. In contrast, roles of vasti and soleus were reversed with the weld (Fig. 5), similar to results observed by Dorn et al. (2012a). Average soleus contribution to upward acceleration also diminished by about 3 m/s² compared to the rolling or point constraints, while average vasti contribution increased comparably (Fig. 5). The rolling and point constraints produced similar mass center accelerations.

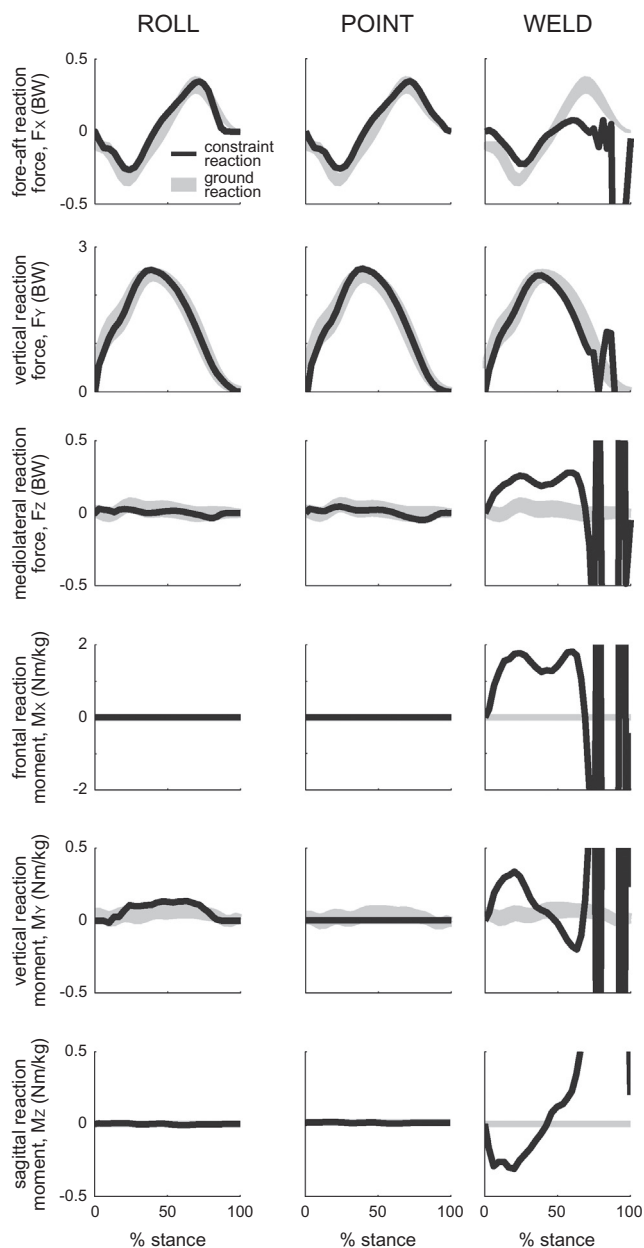


Fig. 4. Comparison of the simulated constraint reaction forces and moments (black) with the experimentally measured ground reaction forces and moments (gray) during simulations of a single subject running using three different constraint types (ROLL, POINT, WELD; see Fig. 2). The shaded region represents the mean \pm one standard deviation of the measured ground reactions over 14 strides.

4. Discussion

The rolling constraint accurately reproduced ground reaction forces and moments during induced acceleration analysis of walking (Liu et al., 2008), running (Hamner et al., 2010), and crouch gait (Steele et al., 2012). In the case of running, the rolling constraint reproduced experimentally measured ground reaction forces and moments more accurately than the point and weld constraints. The rolling constraint produced a moment about the vertical axis because only vertical foot rotation is constrained with respect to ground. Other contact models that limit foot rotations about the frontal and/or sagittal axes (e.g., weld or multiple point constraints) or allow foot rotation about the vertical axis (e.g., point constraint) cannot reproduce the measured ground reaction

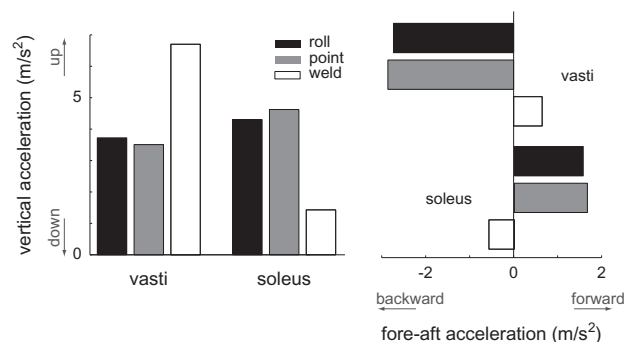


Fig. 5. Comparison of the average contributions of vasti and soleus to upward mass center acceleration (i.e., support) and fore-aft mass center accelerations (i.e., braking and propulsion) during the stance phase of running for three different constraint types (ROLL, POINT, WELD; see Fig. 2) in simulations of a single subject running over 14 consecutive gait cycles.

moment. The vertical ground reaction moment has been shown to significantly affect arm swing during walking and running (Collins et al., 2009; Hinrichs, 1987; Li et al., 2001; Park, 2008), and can affect muscle contributions to mass center and lower extremity joint accelerations through dynamic coupling. Additionally, accurately reproducing the vertical ground reaction moment may be important for understanding pathological gaits, where ground reaction moments are less consistent between subjects. We observed that the weld constraint produces reaction moments much greater than experimentally measured moments and yields vasti and soleus contributions to braking and propulsion in the opposite direction of contributions observed with the rolling or point constraints in analysis of running. Furthermore, the rolling constraint does not require non-physical transition functions necessitated when multiple point constraints are used (Anderson and Pandey, 2003; Dorn et al., 2012a).

As with any model, the rolling constraint has limitations to its accuracy. The constraint utilizes the measured ground reaction force and center of pressure, which will include any errors associated with these experimental measurements. For example, inaccuracy in determining the center of pressure location can occur at the beginning and end of stance as the ground reaction force approaches zero. Additionally, by utilizing the measured center of pressure, the rolling constraint is limited to analyses of measured data and cannot be used in predictive simulations (e.g., Wang et al., 2012). The rolling constraint also represents a rigid connection between foot and ground, which fails to capture deformation of soft tissues during the impact of landing. Therefore, induced acceleration analysis results should be carefully examined during periods of rapid loading and unloading and further testing of rigid constraints should be performed when analyzing movements with impacts, like jumping or cutting. Our models also represent the foot as a single rigid segment, when in reality the foot is a compliant, multiarticular structure. This single segment model is useful for analysis of full-body motions and mass center accelerations, but detailed studies of the foot may require a more complex model.

To have confidence in evaluations of muscle actions derived from muscle-driven simulations, ground contact models should generate forces and moments similar to those measured experimentally. To allow other researchers to assess accuracy of different constraint types we have included an induced acceleration analysis tool with various constraints (e.g., rolling, weld, and point) in OpenSim (Delp et al., 2007; Seth et al., 2011), open source musculoskeletal simulation software. Additionally, to allow others to reproduce and build upon the results of this study, models and data analyzed are freely-available to download from www.simtk.org.

Conflict of interest statement

None of the authors had any financial or personal conflict of interest with regard to this study.

Acknowledgments

We thank Chand John, Jill Higginson, May Liu, and Mike Schwartz for collecting data, creating simulations, and making the results freely available. Samuel Hamner was funded by fellowships from Stanford and NSF. This work was also supported by NIH grants U54 GM072970, R24 HD065690, and R01 HD033929.

References

- Anderson, F.C., Pandy, M.G., 2001. Dynamic optimization of human walking. *Journal of Biomechanical Engineering* 123, 381–390.
- Anderson, F.C., Pandy, M.G., 2003. Individual muscle contributions to support in normal walking. *Gait & Posture* 17, 159–169.
- Collins, S.H., Adamczyk, P.G., Kuo, A.D., 2009. Dynamic arm swinging in human walking. *Proceedings of the Royal Society B: Biological Sciences* 276, 3679–3688.
- Delp, S.L., Anderson, F.C., Arnold, A.S., Loan, P., Habib, A., John, C.T., Guendelman, E., Thelen, D.G., 2007. OpenSim: open-source software to create and analyze dynamic simulations of movement. *IEEE Transactions on Bio-Medical Engineering* 54, 1940–1950.
- Dorn, T.W., Lin, Y.C., Pandy, M.G., 2012a. Estimates of muscle function in human gait depend on how foot-ground contact is modelled. *Computer Methods in Biomechanics and Biomedical Engineering* 15, 657–668.
- Dorn, T.W., Schache, A.G., Pandy, M.G., 2012b. Muscular strategy shift in human running: dependence of running speed on hip and ankle muscle performance. *Journal of Experimental Biology* 215, 1944–1956.
- Hamner, S.R., Seth, A., Delp, S.L., 2010. Muscle contributions to propulsion and support during running. *Journal of Biomechanics* 43, 2709–2716.
- Hinrichs, R.N., 1987. Upper extremity function in running II: angular momentum considerations. *International Journal of Sport Biomechanics* 3, 242–263.
- Kane, T.R., 1961. *Analytical Elements of Mechanics: Dynamics*, 2. Academic Press, New York.
- Kepple, T.M., Siegel, K.L., Stanhope, S.J., 1997. Relative contributions of the lower extremity joint moments to forward progression and support during gait. *Gait & Posture* 6, 1–8.
- Li, Y., Wang, W., Crompton, R.H., Gunther, M.M., 2001. Free vertical moments and transverse forces in human walking and their role in relation to arm-swing. *The Journal of Experimental Biology* 204, 47–58.
- Liu, M.Q., Anderson, F.C., Schwartz, M.H., Delp, S.L., 2008. Muscle contributions to support and progression over a range of walking speeds. *Journal of Biomechanics* 41, 3243–3252.
- Neptune, R.R., Sasaki, K., Kautz, S.A., 2008. The effect of walking speed on muscle function and mechanical energetics. *Gait & posture* 28, 135–143.
- Neptune, R.R., Wright, I.C., van den Bogert, A.J., 2000. A method for numerical simulation of single limb ground contact events: application to heel-toe running. *Computer Methods in Biomechanics and Biomedical Engineering* 3, 321–334.
- Park, J., 2008. Synthesis of natural arm swing motion in human bipedal walking. *Journal of Biomechanics* 41, 1417–1426.
- Peterson, C.L., Hall, A.L., Kautz, S.A., Neptune, R.R., 2010. Pre-swing deficits in forward propulsion, swing initiation and power generation by individual muscles during hemiparetic walking. *Journal of Biomechanics* 43, 2348–2355.
- Sasaki, K., Neptune, R.R., 2006. Differences in muscle function during walking and running at the same speed. *Journal of Biomechanics* 39, 2005–2013.
- Seth, A., Pandy, M.G., 2007. A neuromusculoskeletal tracking method for estimating individual muscle forces in human movement. *Journal of Biomechanics* 40, 356–366.
- Seth, A., Sherman, M., Reinbolt, J.A., Delp, S.L., 2011. OpenSim: a musculoskeletal modeling and simulation framework for in silico investigations and exchange. *Procedia IUTAM*, 2, 212–232.
- Sherman, M.A., Seth, A., Delp, S.L., 2011. Simbody: multibody dynamics for biomedical research. *Procedia IUTAM* 2, 241–261.
- Steele, K.M., Seth, A., Hicks, J.L., Schwartz, M.H., Delp, S.L. Muscle contributions to vertical and fore-aft accelerations are altered in subjects with crouch gait. *Gait & Posture*, <http://dx.doi.org/10.1016/j.gaitpost.2012.10.019>, in press.
- Steele, K.M., Seth, A., Hicks, J.L., Schwartz, M.S., Delp, S.L., 2010. Muscle contributions to support and progression during single-limb stance in crouch gait. *Journal of Biomechanics* 43, 2099–2105.
- Thelen, D.G., Anderson, F.C., Delp, S.L., 2003. Generating dynamic simulations of movement using computed muscle control. *Journal of Biomechanics* 36, 321–328.
- Wang, J.M., Hamner, S.R., Delp, S.L., Koltun, V., 2012. Optimizing locomotion controllers using biologically-based actuators and objectives. *ACM Transactions on Graphics Proceedings of SIGGRAPH* 2012, 31.